ISSN 1674-1056
http://cpb.iphy.ac.cn
http://iopscience.iop.org/cpb
中国物理 B
Chinese Physics
中国物理
Chinese Physics B

Influence of channel length on discharge performance of anode layer Hall thruster studied by particle-in-cell simulation

Xi-Feng Cao(曹希峰), Hui Liu(刘辉), Wen-Jia Jiang(蒋文嘉), Zhong-Xi Ning(宁中喜), Run Li(黎润), Da-Ren Yu(于达仁)

Citation: Chin. Phys. B . 2018, 27(8): 085204. **doi:** 10.1088/1674-1056/27/8/085204

Journal homepage: http://cpb.iphy.ac.cn; http://iopscience.iop.org/cpb

What follows is a list of articles you may be interested in

Influence of a centered dielectric tube on inductively coupled plasma source: Chamber structures and plasma characteristics

Zhen-Hua Bi(毕振华), Yi Hong(洪义), Guang-Jiu Lei(雷光玖), Shuai Wang(王帅), You-Nian Wang(王友年), Dong-Ping Liu(刘东平)

Chin. Phys. B . 2017, 26(7): 075203. **doi:** 10.1088/1674-1056/26/7/075203

Solid-like ablation propulsion generation in nanosecond pulsed laser interaction with carbon-doped glycerol

Zhi-Yuan Zheng(郑志远), Si-Qi Zhang(张思齐), Tian Liang(梁田), Jing Qi(齐婧), Wei-Chong Tang(汤唯冲), Ke Xiao(肖珂), Lu Gao(高禄), Hua Gao(高华), Zi-Li Zhang(张自力)

Chin. Phys. B . 2017, 26(3): 035203. **doi:** 10.1088/1674-1056/26/3/035203

Characteristics of droplets ejected from liquid glycerol doped with carbon in laser ablation propulsion

Zhi-Yuan Zheng(郑志远), Si-Qi Zhang(张思齐), Tian Liang(梁田), Lu Gao(高禄), Hua Gao(高华), Zi-Li Zhang(张自力)

Chin. Phys. B . 2016, 25(4): 045204. **doi:** 10.1088/1674-1056/25/4/045204

Low-frequency oscillations in Hall thrusters

Wei Li-Qiu, Han Liang, Yu Da-Ren, Guo Ning

Chin. Phys. B . 2015, 24(5): 055201. **doi:** 10.1088/1674-1056/24/5/055201

A radial non-uniform helicon equilibrium discharge model

Cheng Yu-Guo, Cheng Mou-Sen, Wang Mo-Ge, Li Xiao-Kang

Chin. Phys. B . 2014, 23(10): 105202. **doi:** 10.1088/1674-1056/23/10/105202

Influence of channel length on discharge performance of anode layer Hall thruster studied by particle-in-cell simulation

Xi-Feng Cao(曹希峰), Hui Liu(刘辉)†, Wen-Jia Jiang(蒋文嘉),
Zhong-Xi Ning(宁中喜)‡, Run Li(黎润), and Da-Ren Yu(于达仁)

Laboratory of Plasma Propulsion, Harbin Institute of Technology (HIT), Harbin 150001, *China*

(Received 22 March 2018; revised manuscript received 23 April 2018; published online 25 July 2018)

Hall thruster has the advantages of simple structure, high specific impulse, high efficiency, and long service life, and so on. It is suitable for spacecraft attitude control, North and South position keeping, and other track tasks. The anode layer Hall thruster is a kind of Hall thruster. The thruster has a longer anode area and a relatively short discharge channel. In this paper, the effect of the channel length on the performance of the anode layer Hall thruster is simulated by the PIC simulation method. The simulation results show that the change of the channel length has significant effect on the plasma parameters, such as potential and plasma density and so on. The ionization region mainly concentrates at the hollow anode outlet position, and can gradually move toward the channel outlet as the channel length decreases. The collision between the ions and the wall increases with the channel length increasing. So the proper shortening of the channel length can increase the life of the thruster. Besides, the results show that there is a best choice of the channel length for obtaining the best performance. In this paper, thruster has the best performance under a channel length of 5 mm.

Keywords: anode layer Hall thruster, channel length, potential

PACS: 52.75.Di, 52.65.–y, 52.65.Pp, 52.65.Rr **DOI:** 10.1088/1674-1056/27/8/085204

1. Introduction

The Hall thruster has the advantages of high specific impulse, long life, compact structure, small volume and less pollution.[1–5] Therefore, it has been gradually noticed and favored in the aerospace field. It has been widely used in satellite station keeping, attitude adjustment, orbit transfer, drag compensation and many interplanetary missions. Hall thruster has an annular channel. The radial magnetic field is formed in the channel due to the inside and outside electric coils and permanent magnet structure. The axial electric field is formed by the potential difference between the anode and the cathode. The electrons are bound by the magnetic field, and the electrons drift along the axis under the orthogonal electromagnetic field. The propellant (usually xenon) is ionized into plasma by electrons, and ions are accelerated to form thrust as shown in Fig. 1.[6] According to the structure and composition, Hall thruster can be divided into two types. One is stationary plasma thruster, its anode area is shorter, the channel structure is longer, the channel wall material is general boron nitride ceramic and other insulation materials; the other is the anode layer Hall thruster, its anode area is longer, the channel is relatively short. The main material for the channel wall of the anode layer Hall thruster is graphite. In experiments, the metal materials such as stainless steel, copper and molybdenum are generally used, and the structure is shown in Fig. 1. Due to the short length of the anode layer Hall thruster channel, the collision between the ions and the wall can be reduced and the life of the thrusters can increase. Therefore, the anode layer thrusters can be used for long-time missions. At present, many researchers have investigated the life of the anode layer Hall thruster, and the main methods of increasing the life are magnetic shielding technology, etc. Compared with stationary plasma thrusters (such as SPT100), the anode layer Hall thruster has a hollow anode structure as shown in Fig. 1. Due to the hollow anode structure, the thruster discharge oscillation can be effectively reduced.[7,8]

Channel wall is an important part of Hall thruster. The change of the channel length has a significant effect on the ionization process and the interaction between particles and wall.[9] And some researches have shown that choosing proper channel length matched with the magnetic field can effectively constrain the neutral gas, improve the utilization of working fluid, make full use of the energy generated by ionization acceleration, improve the ionization and acceleration characteristic, and enhance the thruster performance.[10] Therefore, the research on the influence of the channel length on Hall thruster has an important research value.

Aiming at the influence of anode layer Hall thruster channel length on thruster performance, some researchers have carried out relevant work at present, mainly based on experimental methods. Seiro Yuge *et al.* conducted an experimental study on the influence of the channel length variation and compared the thrust and specific impulse parameters under the conditions of 3 mm and 4 mm in channel length. The results show that the shorter channel length results in lower thrust efficiency and specific impulse.[11] Kimiya Komurasaki

†Corresponding author. E-mail: thruster@126.com
‡Corresponding author. E-mail: ningzx@hit.edu.cn

© 2018 Chinese Physical Society and IOP Publishing Ltd

et al. studied the influence of the channel length on thruster performance under different working conditions. The results show that the acceleration efficiency of ions is the highest when the channel length is 4 mm in Ar environment.[9] Their research focuses on the effect of the channel length on the performance of the thruster. Due to the limitation of experimental measurement, the distribution of the parameters in the channel cannot be obtained. Therefore, the influence of the channel length on the parameters of the anode layer Hall thruster needs to be studied by simulation. For the simulation of the anode layer Hall thruster, the research focuses on the interior of the hollow anode at present. The internal parameter distribution of the hollow anode is adjusted by changing the magnetic field and discharge parameters to try to reduce the effect of the discharge oscillation on the thruster work.[12–16] In previous simulation work, the parameter characteristics in the discharge channel and the hollow anode were described. However, the effect of the channel length on the performance of the thruster was not studied thoroughly.

In this paper, the particle-in-cell simulation method (PIC) is mainly used to simulate and analyze the effect of the channel length on the distribution of parameters. The rest of the paper is organized as follows. In Section 2, a model and magnetic field selection are introduced. In Section 3 the results of numerical simulation results are discussed. Finally, in Section 4 some conclusions are drawn from the present study.

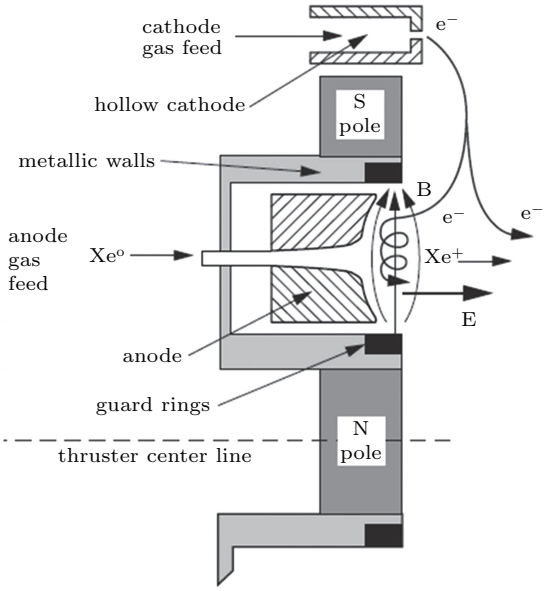


Fig. 1. Anode layer Hall thruster structure diagram.[6]

2. Numerical model

As the thruster is an axisymmetric structure, in this paper we use a two-dimensional (2D) simulation. The simulation area includes the anode, channel, near-field plume area. In the simulation we use the particle-in-cell (PIC) simulation method, which simulates the movement of atoms, electrons and ions. The Monte Carlo method (MCC) is used to simulate the collision between particles. The Poisson equation is used to solve the electric field. The magnetic field generated by plasma is much smaller than the applied magnetic field generated by the coils. So the magnetic field generated by plasma is neglected. This model has been used to study hall thruster,[17,18] high efficiency multistage plasma thrusters,[19] near-wall conductivity,[20] power deposition on the wall and erosion.[21] In the simulation, different boundary conditions need to be considered and different treatment methods are selected for different boundary conditions. The boundary conditions are shown in Fig. 2. The magnetic field used in the simulation is obtained by FEEM software. The design of the general magnetic field is chosen to obtain the peak value of the magnetic field at the channel outlet as shown in Fig. 2.

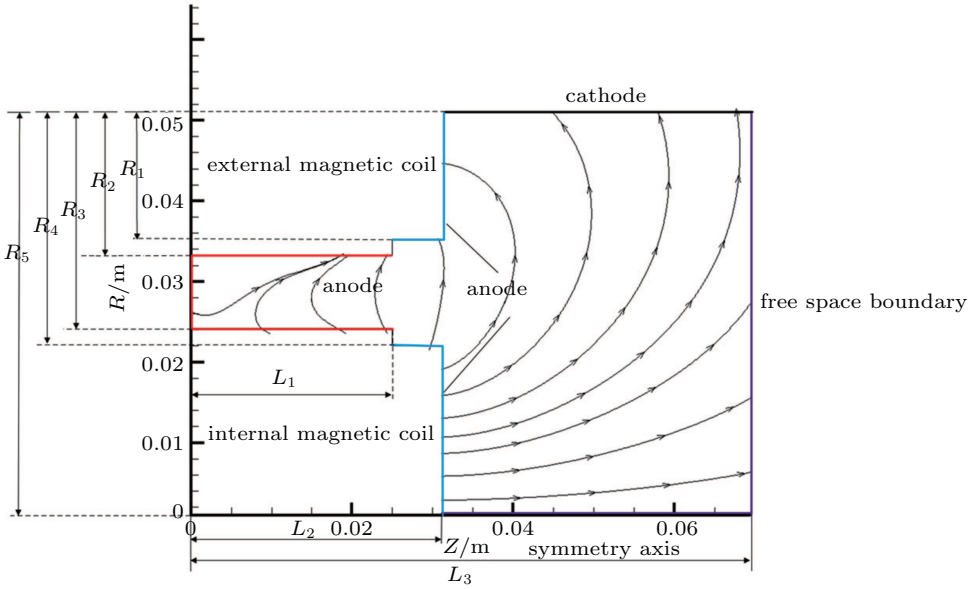


Fig. 2. (color online) Magnetic field distribution and calculation area, including the anode area, channel, near field plume area. Boundary conditions include dielectric, metal, cathode, free space boundary, symmetry axis, metal, dielectric, and anode.

The related parameters are shown in Table 1.

Table 1. Simulation area parameters.

Parameter name	Parameter value
Inner channel radius R_1/mm	21.5
Hollow anode inner diameter R_2/mm	24
Hollow anode outer diameter R_3/mm	31
Outer channel radius R_4/mm	33.5
Simulation area radius R_5/mm	50
Hollow anode length L_1/mm	25
Channel length (L_2–L_1)/mm	2.5∼ 7.0
Simulation area length L_3/mm	50
Anode potential/V	300

The orthogonal grid is used. The size of the grid length is 0.5 mm, which is about 0.5 times the Debye length. The time step Δt equals a smaller value of $0.1\omega_{pe}^{-1}$ and $0.35\omega_c^{-1}$, where ω_{pe} is the electron oscillation frequency and ω_c is the electron cyclotron frequency. Because the electron oscillation is smaller and the value is about 10^{11} Hz, the time step Δt is taken as 10^{-12} s. In order to reduce the computational complexity of the simulation and accelerate the convergence, many researchers have proposed different simulation simplification methods at present.[22–24] In this paper, a simplified model given by Szabo is selected, which increases vacuum permittivity and reduces the ion mass.[25] And the vacuum permittivity is increased by a factor of $\gamma^2 = 1600$, in order to reduce the number of grids and the plasma oscillation frequency. The ion mass is reduced by a factor $1/f = 100$ so that the velocity of the ions increases by $\sqrt{f}$ times to reduce the time scale by the same amount, and the collision cross-section needs to increase by $\sqrt{f}$ times to preserve the density of plasma in the discharge channel. The feasibility of this method has already been proved in our recent simulation work.[26,27] The simulation is calculated by using a personal computer with the above simplified model. After about a three-day calculation, convergent results are obtained successfully.

The change of the channel length is essentially the change of the axial distance between the hollow anode outlet and the channel outlet as shown in Fig. 3. In order to fully consider the effect of the channel length on the performance and parameters of the thruster, the values of channel length L are chosen to be 2.5 mm, 4mmm, 5 mm, 6 mm, and 7 mm, respectively, in this paper.

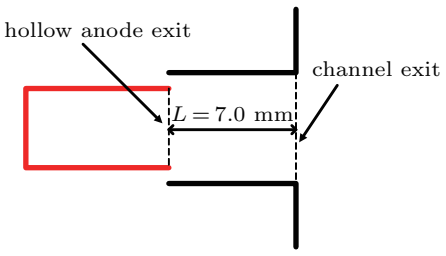


Fig. 3. (color online) Selection of the channel length, $L = 7.0$ mm as an example.

3. Simulation results

3.1. Potential

The distributions of potential in the 5 different cases are similar to each other. Here we only show the distribution of potential under the case of 7 mm as shown in Fig. 4. The simulation results show that the electric potential drop mainly concentrates near the anode outlet, which is consistent with the result obtained in Ref. [16], and significantly different from SPT. The reason is that the wall material of the anode layer Hall thruster is metal material, and the wall is connected with the cathode. There is a significant potential difference between the anode and the wall, which leads to a significant ionization in the area with the potential drop mainly at the anode outlet.

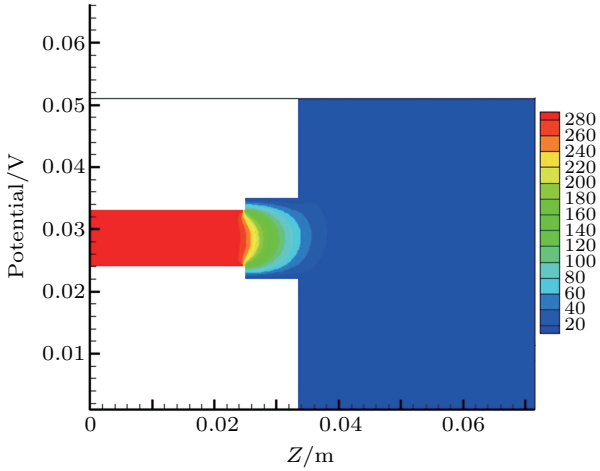


Fig. 4. (color online) Distribution of 2D potential ($L = 7.0$ mm).

Figure 5 shows the distributions of potential along the central axis of the channel under different channel lengths. Under the case of $L = 5.0$ mm, the potential drop mainly concentrates in the channel, and the potential difference between the anode and the channel outlet can reach 280 V. This shows that under the case of $L = 5.0$ mm, the acceleration of ions concentrate in the channel, and a larger ion velocity can be obtained at the outlet position. The binding of the wall-helps to reduce the plume divergence angle. In the case of $L = 7.0$ mm and 6.0 mm, the potential drops in the channel are relatively close and the channel outlet position has a higher potential. This is due to the overlength of the channel that causes a large number of ions to collide with the wall. Meanwhile, the high potential at the outlet position leads to the further acceleration of ions in the plume region, and the increase of the plume divergence angle. Under the case of L =4.0 mm and L =2.5 mm, the potential drops in the channel are further reduced, only 150 V. This result is consistent with the measurement in Ref. [28] . The channel length is 3 mm in the literature. There is also a large potential drop at the anode outlet, and the potential drop in the channel is also 150 V.

This is because the channel length is too short, which leads the ionization region to be near the outlet, resulting in

ionizing a large number of atoms in the plume region. Through the above comparison, it is known that under the condition of $L = 5$ mm, the potential drop in the channel is larger, which contributes to the acceleration of ions.

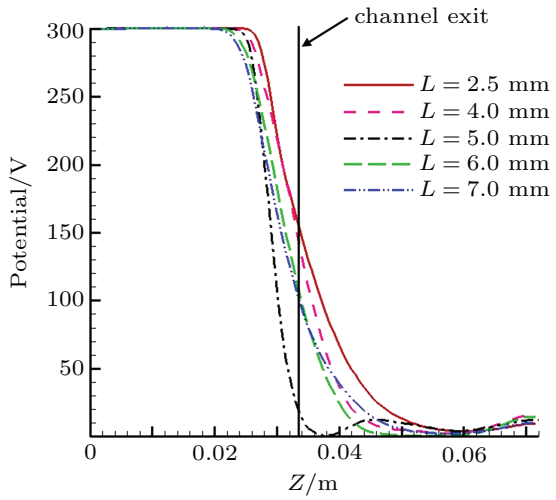


Fig. 5. (color online) Distribution of potential along the central axis of channel.

3.2. Ion density

The 2D distributions of ion density in 5 different cases are similar to each other, here in this work we only show the 2D distribution of ion density under the case of 7 mm as shown in Fig. 6. The ionization zone is mainly near the hollow anode outlet, while the ion density in the downstream area of the anode outlet decreases obviously. The simulation results are in agreement with the results in Ref. [16]. This is because the density of the working gas in the hollow anode is high, and the electron density inside the hollow anode is low that is caused by the wall absorption. The high potential trends the electrons to move to the anode wall. Thus the ionization area is mainly near the hollow anode outlet. Meanwhile, due to the rapid decrease of the potential in the downstream of the anode outlet, the ions have an obvious acceleration which leads to the rapid decrease of the ion density.

For the normal anode structure, due to the fact that the ionization zone is relatively close to the outlet, ions cannot be the ionized and accelerated enough in the short channel. Relatively, the hollow anode structure can effectively bind the ionization zone near the anode outlet. Therefore, the use of hollow anode structure can further shorten the channel length in the application.

Figure 7 shows the distributions of ion density along the central axis of the channel under different channel lengths. In each of the cases of $L = 5.0$ mm and 7.0 mm, the ion density peak is close to $8.5 \times 10^{17}/\mathrm{m}^3$. The peak value is relatively low under the case of $L = 6$ mm. The results are close to the simulation results in Ref. [16]. In the literature, the size and boundary condition of thruster are basically consistent with the conditions adopted in this paper. The simulation results show that the peak value of ion density is located at the hollow anode outlet, and the peak value can reach $1.5 \times 10^{18}/\mathrm{m}^3$, which is close to the result of this paper, so it can also illustrate the accuracy of the simulation in this paper. In each of the cases of $L = 5.0$ mm, 4.0 mm and 2.5 mm, the ion density peak decreases gradually. The reason is that when the channel length is further reduced, the particles cannot be fully ionized, which leads the ionization to decrease. With the channel length shortened, the peak position shifts towards the outlet position from the peak position, which means that the ionization zone moves along the outlet position.

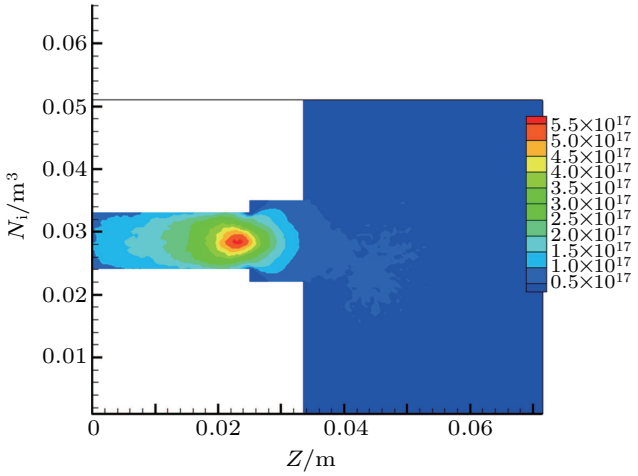


Fig. 6. (color online) 2D ion number density distribution ($L = 7.0$ mm).

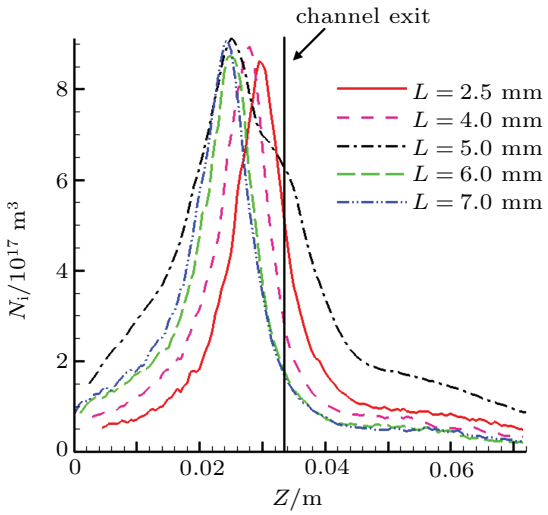


Fig. 7. (color online) Distributions of ion number density along central axis of channel for different channel lengths.

3.3. Ion flux

Ion flux is an important parameter that affects the performance of the thruster. There is a large potential difference between the anode and the channel wall, which causes the ions to obtain a large radial velocity. At the wall position, ions have a significant influence on the wall surface. Under long-term ion scour, the wall surface of the thruster will be seriously eroded.

And at the same time ion scour will cause ion energy loss, and thus degrading the performance of the thruster.

With the different channel lengths, the distributions of ion flux at the wall for different channel lengths are shown in Fig. 8. By comparison, expect the case of $L = 2.5$ mm, the ion flux on the wall basically first increases and then decreases. This is because there is a big potential difference between the anode outlet and the wall, and ions impact the wall in a certain direction. By comparison, it is found that the position of the peak value of ions flux gradually moves towards the outlet as the channel becomes shorter. When $L = 2.5$ mm, the region of high ion flux shifts to the plume region. The ion deposition rate at the wall is further calculated on the wall of the channel, and the results are shown in Fig. 9. The statistical results show that when $L = 5.0$ mm, the maximum ion deposition rate is 5.27×10^{15}/s, and the ion deposition rate is 6.59 times that in the case of $L = 2.5$ mm. This is due to the higher ion density in the channel in the case of $L = 5.0$ mm as shown in Fig. 7. Meanwhile, the area with the higher ion flux shifts to the plume area in the case of $L = 2.5$ mm. So there occurs a large difference between the two cases. Therefore, by appropriately shortening the channel length, the wall loss is reduced.

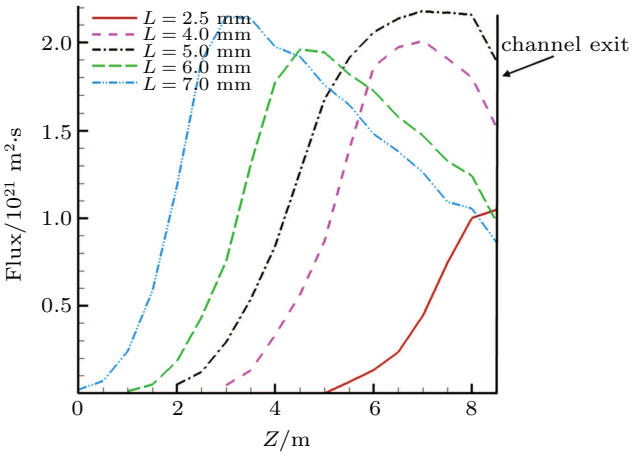


Fig. 8. (color online) Ion flux at channel wall for five channel lengths.

Further, the statistics of the ion energy at the wall surface shows that as the channel length increases, the ion energy deposition rate on the wall surface increases. Through the simulation results in Subsection 3.2, we can see that the main ionization region is located at the anode outlet. Meanwhile, as shown in Fig. 7, the ion density peaks are relatively close in the case of $L = 5.0$ mm, 6.0 mm, and 7.0 mm. In the case of $L = 7.0$ mm, the reason for the more ion energy deposition is that the channel is longer and more ions collide with the wall. In the case of $L = 2.5$ mm and $L = 4.0$ mm, the channel is shorter, the collision between the ions and the wall becomes less, and the energy deposition is relatively low. So in the case of the longer channel, the ion energy deposition at the wall surface is larger, which indicates that the ion energy loss is relatively large, which further shows that the overlong channel has a negative effect on the performance of the thruster.

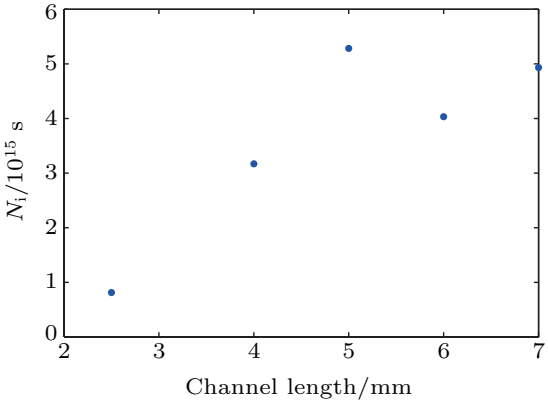


Fig. 9. (color online) Total ion deposition rate on the channel wall versus channel length for five channel lengths.

4. Conclusions

In this paper, we simulate and analyze the effect of the channel length on the distribution of the parameters in the anode layer Hall thruster channel and near field plume area by PIC simulation method. Through the analysis of the electric potential, the potential gradient and the potential drop in the channel are maximum in the case of 5 mm in channel length, which shows that the performance of the thruster is optimal at this length.

By comparison with the distribution of ion density, the hollow anode structure can effectively confine the ionization zone near the anode outlet. And with the shortening of the channel length, the ionization zone shifts towards the channel outlet. As the channel becomes longer, the ion loss increases obviously, and the ion density at the outlet position is low. As the channel becomes shorter, the ions cannot be fully accelerated, the ion density peak significantly decreases, and the performance of the thruster decreases significantly. By analyzing the ion flux and ion energy deposition on the wall, the total influence of ions on the wall is stronger under the longer channel conditions, which has a negative effect on the life of the thruster. Appropriately, shortening the channel length increases the life of the thruster.

In summary, the channel length has a significant effect on the discharge process of the anode layer Hall thruster, and the comparison results show that there is an optimal channel length to achieve the best performance. Under this condition discussed in this paper, the thruster performance is optimal when the channel length is 5 mm.

References

[1] Mazouffre S 2016 *Plasma Sources Sci. Technol.* **25** 033002
[2] Boeuf J P 2017 *J. Appl. Phys.* **121** 011101

[3] Kim H, Choe W, Lim Y, Lee S and Park S 2017 *Appl. Phys. Lett.* **110** 114101

[4] Yu D R, Qing S W, Wang X G, Ding Y J and Duan P 2011 *Acta Phys. Sin.* **60** 025204 (in Chinese)

[5] Duan P, Qin H J, Zhou X W, Cao A N, Chen L and Gao H 2014 *Chin. Phys. B* **23** 075203

[6] Goebel D M, Hofer R R, Mikellides I G, Katz I, Polk J E and Dotson B 2015 *IEEE Trans. Plasma Sci.* **43** 118

[7] Yuge S and Tahara H 2005 *The 29th International Electric Propulsion Conference*, October 31–November 4, 2005, Princeton, USA, IEPC-2005-020

[8] Wei L Q, Han L, Yu D R and Guo N 2015 *Chin. Phys. B* **24** 055201

[9] Komurasaki K, Mikami K and Kusamoto D 1996 *The 32nd Aiaa/sae/asee Joint Propulsion Conference*, July 1–3, 1996, Florida, USA, AIAA-96-3194

[10] Ding Y, Jia B Y, Sun H Z, Wei L Q, Peng W J, Li P and Yu D R 2018 *Adv. Space Res.* **61** 837

[11] Yuge S, Kuwamura Y and Tahara H 2007 *The 30th International Electric Propulsion Conference*, September, 17–20 2007, Florence, Italy, IEPC-2007-336

[12] Kubota K, Oshio Y, Watanabe H, Cho S, Ohkawa Y and Funaki I 2016 *The 52nd Aiaa/sae/asee Joint Propulsion Conference*, July 25–27, 2016, Utah, USA, AIAA-2016-4628

[13] Mikellides I G, Katz I, Goebel D M and Jameson K K 2007 *J. Appl. Phys.* **101** 063301

[14] Katz I, Anderson J R, Polk J E and Brophy J R 2003 *J. Propul. Power* **19** 595

[15] Fujita D, Kawashima R, Ito Y, Akagi S, Suzuki J, Schonherr T, Koizumi H and Komurasaki K 2014 *Vacuum* **110** 159

[16] Yokata S, Komurasaki K and Arakawa Y 2006 *The 42nd Aiaa/sae/asee Joint Propulsion Conference*, August 21–24, 2006, Colorado, USA, AIAA-2006-5170

[17] Liu H, Yu D R, Yan G J and Liu J Y 2008 *Contrib. Plasma Phys.* **48** 603

[18] Liang S T, Liu H and Yu D R 2018 *Chin. Phys. B* **27** 045201

[19] Liu H, Chen P B, Sun Q Q, Hu P, Meng Y C, Mao W and Yu D R 2016 *Acta Astronaut.* **126** 35

[20] Yu D, Li H, Wu Z and Mao W 2007 *Phys. Plasmas* **14** 064505

[21] Cao X F, Hang G R, Liu H and Yu D R 2017 *Plasma Sci. Technol.* **19** 105501

[22] Fox J M 2007 "Advances in fully-kinetic PIC simulations of a near-vacuum Hall thruster and other plasma systems", Ph. D. dissertation (Boston: Massachusetts Institute of Technology)

[23] Fife J M 1999 "Hybrid-PIC modeling and electrostatic probe survey of Hall thrusters", Ph. D. dissertation (Boston: Massachusetts Institute of Technology)

[24] Parra F I, Ahedo E, Fife J M and Martínezsánchez M 2006 *J. Appl. Phys.* **100** 023304

[25] Szabo J J 2001 "Fully kinetic numerical modeling of a plasma thruster", Ph. D. dissertation (Boston: Massachusetts Institute of Technology)

[26] Zhao Y J, Liu H, Yu D R, Hu P and Wu H 2014 *J. Phys. D: Appl. Phys.* **47** 045201

[27] Liu H, Cheng P B, Zhao Y J and Yu D R 2015 *Chin. Phys. B* **24** 085202

[28] Yuge S, Hara K, Cho S, Takahashi D, Komurasaki K and Arkawa Y 2009 *The 31th International Electric Propulsion Conference*, September 20–24, 2009, Michigan, USA, IEPC-2009-149